INVESTIGATING ADSORPTION ISOTHERMS AND KINETICS, AND ECOTOXICITY OF ACTIVATED CARBON FROM CARBON-FIBER REINFORCED POLYMER (CFRP)

NIK MISHA ADRINA NIK AHMAD SHAFRIZAL[1], RICCA RAHMAN NASARUDDIN[1*], MARIATUL FADZILLAH MANSOR[1], NOR FARAH HUDA ABD HALIM[2]

[1]Department of Chemical Engineering & Sustainability, Kulliyyah of Engineering, International Islamic University. Malaysia (IIUM), Jalan Gombak, 53100 Kuala Lumpur, Malaysia.

[2]Department of Materials and Manufacturing Engineering, Kulliyyah of Engineering, International Islamic University. Malaysia (IIUM), Jalan Gombak, 53100 Kuala Lumpur, Malaysia.

**Corresponding author: riccanasaruddin@iium.edu.my*

ABSTRACT: This study presents the synthesis of activated carbon (AC) from carbon fiber reinforced polymer (CFRP) waste as a sustainable adsorbent for wastewater treatment. Characterization by FTIR, SEM, and XRD confirmed the development of functional groups, a porous morphology, and a predominantly amorphous carbon structure in AC, with minor graphitic domains in CFRP. Adsorption tests using the methylene blue (MB) dye showed good performance, with the Langmuir isotherm resulting in the best-fitted model (adjusted R^2 = 0.88), indicating monolayer adsorption and pseudo-first-order kinetics (adjusted R^2 = 0.96). Thus, confirming concentration-dependent adsorption of MB by AC, produced from CFRP. Ecotoxicity evaluation using brine shrimp assay revealed an LC_{50} of 33.11 mg (or 3311 mg/L), suggesting moderate toxicity. These findings demonstrate that AC derived from CFRP exhibits strong adsorption efficiency with acceptable ecological risk, providing a viable pathway to convert CFRP waste into valuable materials for environmental remediation.

KEYWORDS: *Carbon fiber reinforced polymer, Activated carbon, Langmuir isotherm, Ecotoxicity, and Methylene Blue.*

1. INTRODUCTION

Over the past decade, demand for carbon fiber-reinforced polymer (CFRP) has surged due to its numerous desirable qualities, making it a leading material in modern engineering and manufacturing. CFRP's exceptional strength-to-weight ratio, corrosion resistance, and directional strength make it ideal for aerospace, automotive, marine, and chemical engineering applications [1]. Despite its benefits, recycling CFRP is challenging due to its heterogeneous nature, leading to a focus on converting its waste into value-added products [2]. The global carbon fiber industry has grown significantly, with production reaching 28,000 tons in 2006 and a market value of up to 5.6 billion US dollars [3]. However, the disposal of CFRP in landfills is no longer an option due to legal, economic, and environmental concerns, prompting research into sustainable recycling methods [4].

Therefore, it is imperative to explore alternative solutions that can mitigate the environmental impact of CFRP waste. Converting waste into value-added products has been a popular focus in engineering and research fields these days [5]. One promising solution under this scope is converting CFRP into activated carbon (AC), a material known for its high surface area and superior adsorption properties.

It is no longer a secret that AC is in high demand these days, especially in the chemical industry. It is well-known for its ability to filter contaminants from water and air, among many other uses. From that revelation, AC has mostly been used as an adsorbent, especially at wastewater treatment plants [6]. In the wastewater treatment systems, the adsorption technology of AC is typically used in the primary treatment, water purification process, or finally in the advanced treatment process [7]. Usually, the production of AC was done using biomass wastes [6] and a limited study utilizes CFRP as the raw material for AC production. Therefore, it is worthwhile to utilize CFRP for the AC production. Pyrolysis is typically used to convert CFRP into AC. At high temperatures, AC is synthesized after calcination.

Furthermore, assessing the ecotoxicity of the resulting AC is crucial to ensure that its use does not introduce new environmental hazards. Conducting ecotoxicity tests, such as determining the LC_{50}, enables us to evaluate the potential impact of CFRP-derived AC on aquatic life and verify compliance with environmental safety standards. This comprehensive evaluation aims to provide a clear understanding of the ecological and functional benefits of converting CFRP into AC, thereby contributing to more sustainable waste management practices and environmental remediation strategies.

Therefore, in this study, AC was produced from CFRP. Then the adsorption test was done to evaluate the functionality of AC as an adsorbent because this application is mostly effective in removing adsorbate from wastewater and producing high-quality water [8]. The adsorption properties, focusing on the adsorption isotherm and adsorption kinetics, were determined to understand the adsorption mechanism of the CFRP-derived AC. Then, an ecotoxicity test, such as computing the LC_{50} value, was also conducted to assess the safety, risk, and impact of CFRP-derived AC on aquatic ecosystems.

2. MATERIALS AND METHODS

2.1. Preparation of Materials

The CFRP waste powder generated from the machining or milling of cured CFRP laminates was sourced from ongoing CFRP research activities within the Department of Materials and Manufacturing Engineering at the International Islamic University Malaysia (IIUM), which ensured consistent availability and a well-defined processing history. The CFRP powder was thoroughly cleaned and prepared before use. Potassium hydroxide (KOH), the activating agent, was purchased from a local supplier (Chemistree Sdn. Bhd.) via an online marketplace (Lazada). The KOH was 98% pure and at soap-production grade. Nitric acid (HNO_3) in ACS reagent grade (70% v/v) was purchased from Sigma-Aldrich-Merck. Deionized (DI) water was used as the solvent in all the experiments to ensure high purity. Methylene blue (MB) powder (Bendosen brand, 100% purity) was purchased from a local supplier (A&D World Enterprise) via an online marketplace (Shopee). For ecotoxicity testing, brine shrimp eggs (*Artemia* sp.) and artificial sea salt were used to prepare the saline solution needed to maintain the eggs. The *Artemia* sp. nauplii (also called cysts) and sea salts for the making of artificial seawater were purchased from VL Aquatic shop, Kuala Lumpur, Malaysia.

2.2. Synthesis of activated carbon from CFRP

CFRP powder was mixed with KOH in a 1:1 mass ratio and deionized water according to a previous study [8]. The resulting mixture was first dried in an air fryer at approximately 100 °C for 30 minutes to remove residual moisture. After drying, the sample was subjected to calcination and chemical activation in a furnace at 600 °C for one hour in the presence of KOH. The resulting product was acid-washed with 5% HNO_3, rinsed with DI water until neutral pH, and dried overnight to remove moisture. Comprehensive characterization of CFRP-derived AC was conducted using several techniques. Fourier Transform Infrared Spectroscopy (FTIR) was employed to identify surface functional groups, while Scanning Electron Microscopy (SEM) provides insights into surface morphology and pore structure of the AC. In addition, X-ray Diffraction (XRD) was used to analyze the crystalline or amorphous phases of the AC.

2.3. Adsorption isotherm test

In the adsorption isotherm test, 20 mg of AC was accurately weighed and placed into microcentrifuge vials (2 mL). MB solutions (1.5 mL) of different concentrations (100, 200, 300, 400, and 500 mg/L) were added into the vials, and they were then centrifuged at 700 rpm for 10 minutes to ensure thorough mixing and adsorption. The experiment was conducted in triplicate for each concentration to ensure reproducibility and accuracy. After centrifugation, the supernatant was carefully pipetted into cuvettes for absorbance measurement. The absorbance spectrum for each solution was plotted to confirm the peak absorbance wavelength, and the peak absorbance was measured at 659 nm using a UV-Vis spectrophotometer. This method allowed the determination of the AC adsorption capacity by analyzing the reduction in MB concentration in solution.

The amount of MB adsorbed onto the surface of the AC was calculated using the following equation (1):

$$q_e = \frac{(C_{O-}\ C_f)V}{m} \tag{1}$$

where q_e represents the adsorption capacity at equilibrium (mg/mg), which means mg of adsorbate per mg of adsorbent (AC). Meanwhile, V represents the volume of the MB solution (L) and m represents the mass of adsorbent (mg). In this adsorption study, the Langmuir and the Freundlich isotherm models were used to fit the results obtained from investigating the effects of initial dye concentration. The following isotherms were exploited.

Langmuir isotherm model:

$$q_e = \frac{q_m K_L C_e}{1+ K_L C_e} \tag{2}$$

Freundlich isotherm model:

$$q_e = K_F {C_e}^{1/n} \tag{3}$$

Goodness-of-fit was evaluated by comparing R^2 values and various statistical indices which can be obtained by the following relations:

$$R^2 = 1 - \frac{\sum (q_{e,\exp} - q_{e,cal})^2}{\sum (q_{e,\exp} - q_{e,mean})^2} \tag{4}$$

where $q_{e,\exp}$, $q_{e,mean}$ and $q_{e,cal}$ are the experimental adsorption capacity (mg/mg), calculated adsorption capacity predicted from the isotherm model (mg/mg) and the average value of the experimental adsorption capacity (mg/mg) for triplicates, respectively. To evaluate each adsorption isotherm model's fitness, the regression coefficient (R^2) is employed as a criterion [9].

2.4. Adsorption kinetics testing

For the adsorption kinetic study, 20 mg of AC was accurately weighed and placed into microcentrifuge vials. Methylene blue (MB) solutions at 300 mg/L were added, and the vials were centrifuged at 700 rpm for 10 minutes to ensure thorough mixing and adsorption. The experiment was conducted in triplicate for each MB concentration to ensure reproducibility and accuracy. Absorbance was measured using a UV-Vis spectrophotometer at 659 nm, with readings taken every 10 minutes over 90 minutes. This approach enabled the determination of AC's adsorption capacity by analyzing the decrease in MB concentration in solutions. The following models were used for kinetic studies.

Arrhenius zero-order kinetic model:

$$[C_t]=-kt+[C]_0 \tag{5}$$

Arrhenius first-order kinetic model:

$$\ln [C_t]=-kt+ln[C]_0 \tag{6}$$

Arrhenius second-order kinetic model:

$$1/[C_t]=-kt+1/[C]_0 \tag{7}$$

where $[C]_0$ and $[C_t]$ is the initial and final concentration of the MB solution, k is the reaction rate constant (m/s), and t is time (minutes). The concentration of MB was determined from the UV–Vis absorbance values of the initial and post-adsorption solutions, using the Beer–Lambert law to relate absorbance intensity to MB concentration [10].

2.5. Ecotoxicity test using brine shrimp assay

The ecotoxicity test using the brine shrimp assay comprises two key steps. First, a brine shrimp hatchery was created. Artificial seawater was made by mixing one tablespoon of sea salt with a pinch of bicarbonate of soda to adjust the pH. A tablespoon of brine shrimp cysts was introduced into the mixture. Aeration was provided by a pump connected to the hatchery via a tube. Second, for the lethality testing, hatched brine shrimp were placed in containers with artificial seawater and different doses of AC (20, 30, and 50 mg). A negative control with distilled water and a positive control with formalin solution, each containing 20 hatched brine shrimp, were also included. The containers were incubated in a well-lit area at a stable temperature of 25 °C to 30 °C. After 24 hours, the number of brine shrimp surviving in each container was counted to assess the effects of the AC doses. The percentage of survivability in each concentration was calculated. Lethality tests were verified using the following equation:

$$\text{Percentage Lethality} = \left(\frac{\text{Total Number of Organisms}}{\text{Number of Dead Organisms}}\right) \times 100\% \tag{11}$$

3. RESULTS AND DISCUSSION

3.1. Synthesis and Characterization of AC

The overall yield of AC from CFRP was 47.5 wt.%, indicating that nearly half of the precursor material was successfully converted into a carbon-rich product. This yield is considered reasonable for carbonization-based processes, as significant mass loss typically occurs due to the removal of volatile components, decomposition of polymeric matrices, and elimination of non-carbon elements during calcination. The obtained value also reflects the dense, stable structure of CFRP, which differs from biomass-based precursors such as coconut shells or wood, where yields are often lower due to their higher volatile content [8]. A yield of this magnitude suggests that CFRP is a viable precursor for AC production, offering both material recovery and potential scalability for practical applications such as wastewater treatment.

Then, the synthesized AC derived from CFRP waste was characterized and compared with untreated CFRP waste to determine its physicochemical properties. The first characterization was to determine the functional groups of the AC using FTIR analysis. Based on the FTIR results in Fig. 1, the regions i, ii, iii, iv, and v indicate the existence of hydroxyl O-H stretching, alkanes C-H stretching, CO_2 stretching, aromatic C=C stretching, and C-O stretching, respectively. There is a clear indication that AC has a higher peak intensity in regions ii and iii. In comparison, CFRP shows higher peak intensities in regions i, iv, and v, with the peak at i (at a wavenumber of 3505 cm^{-1}) indicating successful activation of the CFRP with nitric acid, which introduced additional hydroxyl (-OH) functional groups. Intensity at region iii indicates CO_2 trapped in pores of synthesized AC, which could be due to the method of handling and storage or the adsorption of the CO_2 gas on the AC surface [11]. Table 1 further describes the interpretation of the FTIR results by assigning possible functional groups to peaks at specific wavenumbers.

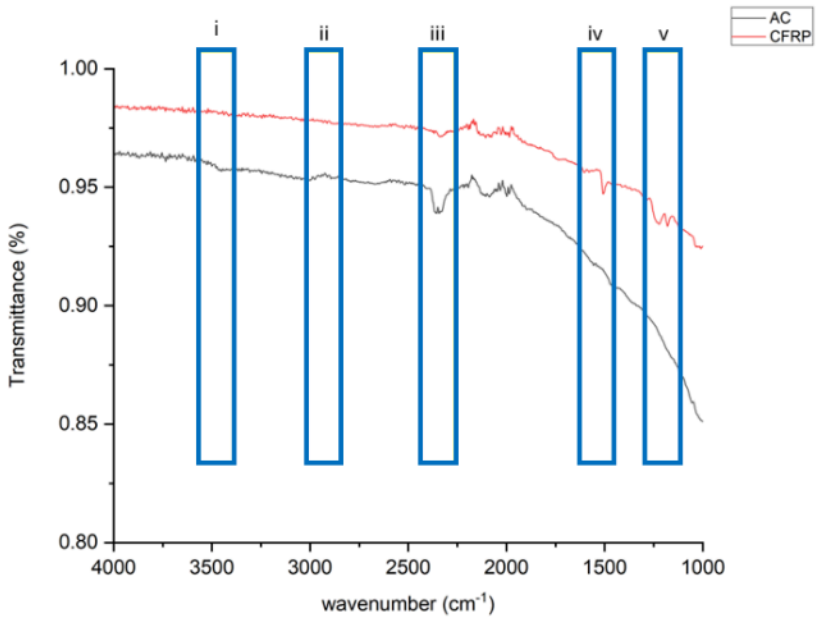

Fig. 1. FTIR spectra of the raw CFRP material and the AC synthesized from CFRP, showing the functional groups before and after activation.

Table 1: Functional groups interpretation from the peaks in the FTIR spectra in Fig. 1

Actual wavenumber [cm^{-1}]	Range of wavenumber [cm^{-1}]	Possible functional groups
1183	1000-1100	C-O stretching
1510	1400-1620	Aromatic C=C stretching
2173	2100-2200	Alkanes C=C stretching
2354	2300-2400	Alkyne C≡C, Aromatic Nitrile C≡N, CO_2
2950	2800-3300	Alkanes C-H stretching, Alkenes C=H stretching
3505	3200-3700	Hydroxyl groups (O-H) stretching

The structure of the AC was further characterized using XRD (Fig. 2). Based on the results in Fig. 2(a), the broad peaks in the XRD pattern of AC indicated a largely amorphous structure with a high degree of disorder, typical for AC synthesized using other agricultural wastes. The prominent peak around 2θ = 25 – 30 degrees corresponded to the (002) plane of graphitic carbon, suggesting the presence of graphitic domains [12,13]. Additionally, a smaller, broader peak around 2θ = 40–50 degrees likely corresponded to the (100) plane, indicating less-ordered graphitic carbon structures. The obtained XRD patterns are well-matched with the standard pattern for the activated carbon (ICDD No. 41–1487) [14]. Overall, the XRD pattern of the AC indicated that it was primarily amorphous, with some graphitic regions, reflecting a typical disordered structure with areas of graphitization.

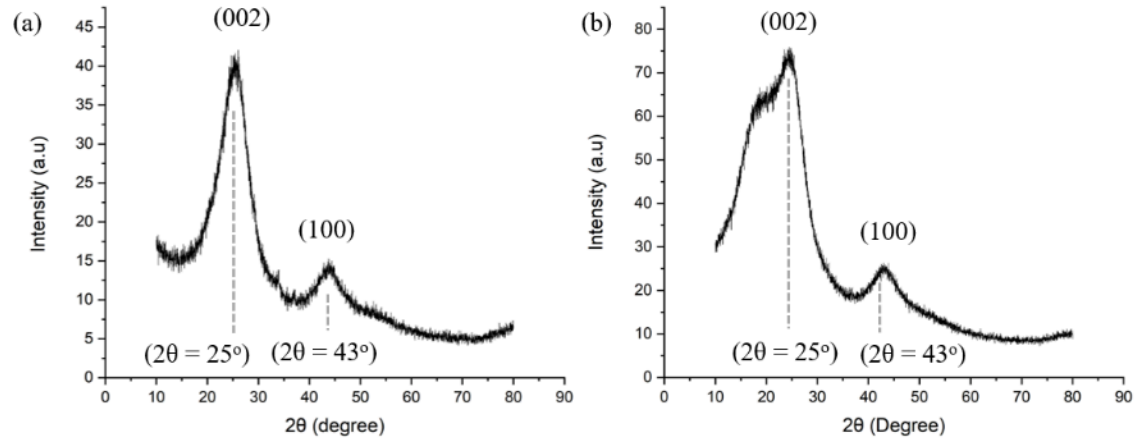

Fig. 2. The X-ray diffraction (XRD) patterns of (a) AC and (b) CFRP waste.

The presence of graphite could influence the pore size distribution, with graphitic regions contributing to the formation of mesopores (2-50 nm) rather than micropores (<2 nm), which could be beneficial for adsorbing larger molecules. In addition, the CFRP peak

is stronger and more intense than that of AC. At 2θ = 25°, CFRP has ≈ 80 a.u. compared to ≈ 40 a.u. for AC. Meanwhile, at 2θ = 43°, associated with the (100) plane, indicating the presence of crystalline graphitic carbon fibers [12,14]. The peak for the CFRP is also higher (≈ 25 a.u.) than that of AC (≈ 14 a.u.), suggesting that CFRP has greater crystallinity due to its structured fiber content. Following calcination and activation, the resulting AC consists primarily of disordered, porous carbon with significantly reduced crystallinity, rendering it more amorphous than the original CFRP material.

SEM was employed to analyze the surface topology, morphology, and porosity of the substrates, which are crucial factors in adsorption studies. SEM is particularly effective for characterizing sorbents because it can detect features as small as 1 nm. This capability enables detailed visualization of micropores in SEM micrographs. Fig. 3(a) presents the SEM image of AC produced from CFRP waste at a magnification of x500. At this magnification, the structure exhibits a porous, irregular morphology with a network-like framework. The material contains interconnected pores and fractured surfaces resulting from high-temperature thermal treatment. Elongated fragments and voids are also visible, indicating some retention of the carbon fiber backbone, which may contribute to structural stability and the formation of open channels for adsorption [10].

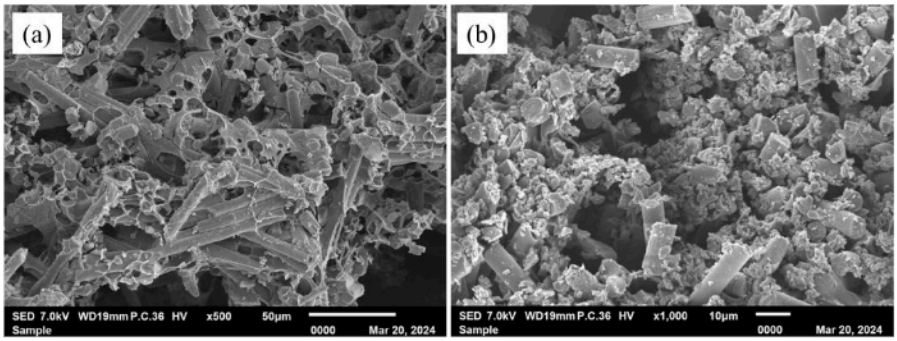

Fig. 3. SEM images of AC synthesized from CFRP waste with (a) x500 and (b) x1000 magnifications.

The use of KOH as a chemical activator resulted in increased pore formation. It altered the CFRP fibers' structure from elongated to smaller components with finer pores, as shown in the SEM image in Fig. 3(b). At elevated temperatures, KOH reacts with carbon to generate potassium compounds (e.g., K, K_2O, K_2CO_3) that diffuse into the carbon lattice [8,10]. Cooling and leaching remove these compounds, creating new voids and channels that etch the carbon framework and produce many micropores and mesopores. The finer structures and smaller pores observed in Fig. 3(b) confirm that KOH activation promotes fragmentation of the CFRP waste into highly porous carbon with a rough surface texture. Such pore development is critical for adsorption applications, as it increases the available surface area and enhances pollutant accessibility [13].

The nitric acid (HNO_3) washing also improved the visibility of the pore structure by dissolving residual inorganic species and metallic potassium trapped within the carbon framework. This step not only cleanses blocked pores, thereby improving pore accessibility, but also opens additional microporous channels by removing deposits lodged in the pore walls. As a result, the final AC demonstrates a more open and accessible pore network, which directly contributes to its adsorption capacity in wastewater treatment [10].

3.2. Adsorption isotherm

Numerous adsorbates have been employed in recent studies to investigate the adsorption isotherms of AC, including Rhodamine B [15], methyl red and methyl orange dyes [9], an azo dye [16], and methylene blue (MB) [17]. However, this study focuses explicitly on MB because it offers several advantages as a model adsorbate. It is widely used in adsorption research due to its well-defined molecular structure, strong UV-Vis absorbance, and high-water solubility, which enable accurate quantification and reproducible measurements. MB is also a common pollutant from textile, paper, and dye industries, making it suitable for testing [10]. Our previous study also found that the AC synthesized from CFRP waste effectively removes MB from water [10]. Understanding the adsorption isotherm helps elucidate the mechanism and optimize synthesis to improve AC performance.

In addition, the adsorption of MB can be conveniently monitored through a distinct color change in the solution. Initially, MB imparts a deep blue color to the aqueous phase. However, as adsorption progresses, the dye molecules bind to the AC surface via electrostatic attraction, π–π interactions, and pore-filling mechanisms [18]. Once most MB molecules adsorbed on AC were removed from solution, the blue color gradually faded and eventually became nearly colorless, indicating that adsorption sites on the AC were saturated and equilibrium was reached, as shown in Fig. 4(a). This visual change not only provides a straightforward qualitative indicator of adsorption efficiency but can also be quantified by measuring absorbance reduction at the characteristic MB wavelength (around 664 nm) using UV–Vis spectrophotometry [10].

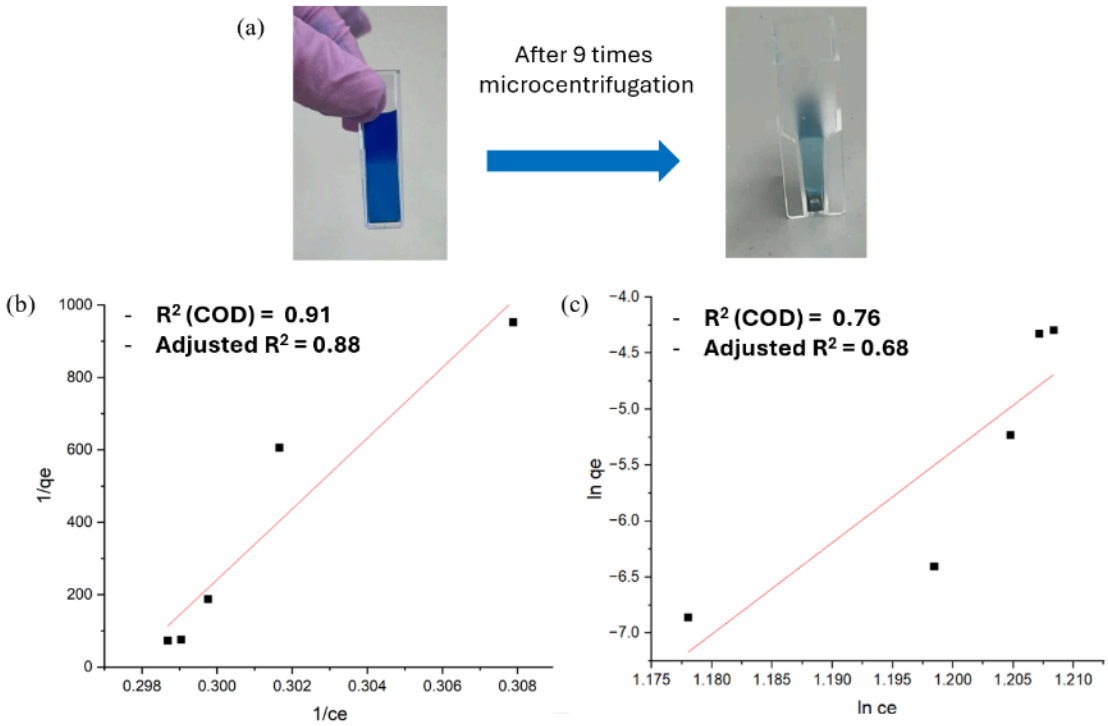

Fig. 4. (a) Photographs of the MB solution (300 mg/L) before adsorption and after nine cycles of microcentrifugation with AC, (b) Langmuir isotherm plot showing the linear fit of $1/q_e$ versus $1/C_e$, and (c) Freundlich isotherm plot showing the linear fit of ln q_e versus ln C_e.

Fig. 4 also demonstrates distinct variations in how different isotherm models characterize MB adsorption onto AC. When evaluating the goodness-of-fit of adsorption isotherm and kinetic models, both the coefficient of determination (R^2) and the adjusted R^2 can be considered. R^2 indicates the proportion of variance explained by the model and helps assess simple single-parameter fits. However, it always increases with additional parameters, even if the model does not truly improve. Adjusted R^2, on the other hand, compensates for the number of model parameters and provides a more reliable measure when comparing models of different complexities. Therefore, while R^2 is adequate for evaluating individual model fits, adjusted R^2 is preferred when comparing multiple models with varying numbers of parameters to avoid overestimating the quality of fit [16]. Linear regression analysis is used for model selection and supports the Langmuir model for this application. The Langmuir model assumes monolayer adsorption and a uniform surface with specific sites for MB adsorption on the synthesized AC, which describes the interaction mechanism. This model posits that adsorption occurs at specific, identical, and equivalent localized sites. It also assumes there is no steric hindrance or lateral interaction between adsorbed molecules, even on adjacent sites [19]. In contrast, the Freundlich isotherm suggests surface heterogeneity, whereas the Langmuir model better describes the adsorption process in this context [16].

3.3. Adsorption kinetics

From Fig. 5, it is evident that MB adsorption onto AC synthesized from CFRP follows a first-order Arrhenius model, with an adjusted R^2 of 0.96. While the Arrhenius second-order model is also a good fit, the first-order model offers a superior fit, with a higher adjusted R^2 than the second-order model ($R^2 = 0.92$). The left-hand region in the graphs in Fig. 5 shows a plateau trend before any change, indicating an induction period with little or no adsorption. During this phase, adsorbate molecules interact with the adsorbent surface but are not yet taken up in significant amounts. This delay may result from the time needed for MB molecules to reach adsorption sites or to overcome an activation energy barrier.

Once adsorption begins, the process typically enters a relatively rapid phase, indicating interaction between MB and AC after the induction period. Several factors may account for the induction phase. The surface of AC is often modified to increase its adsorption capacity; functional groups such as hydroxyl (-OH), carboxyl (-COOH), and carbonyl (-C=O) are commonly present on the surface and can form hydrogen bonds or participate in other interactions with adsorbate molecules. This is supported by the detection of hydroxyl (-OH) groups in FTIR spectra during AC characterization. Another explanation for adsorption initiation is the presence of weak Van der Waals forces between the adsorbate molecules and the carbon surface. These forces result from transient dipoles within the adsorbate molecules, induced by the electric field generated by the carbon surface.

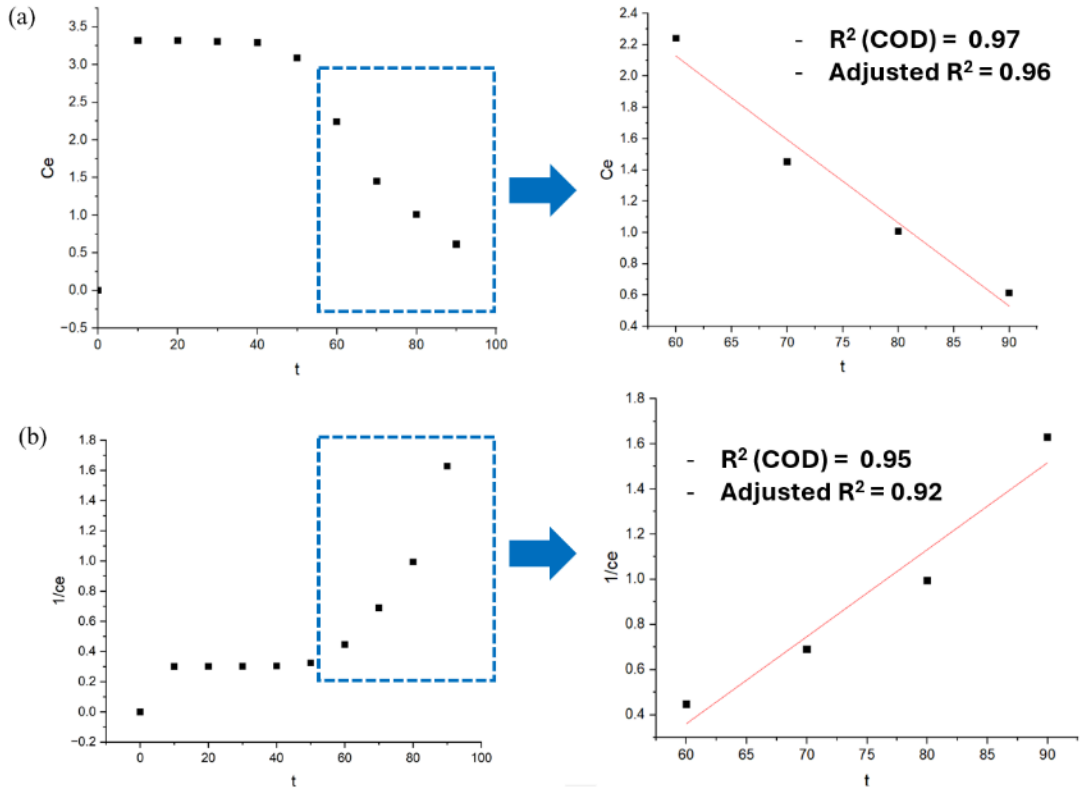

Fig. 5. Arrhenius (a) first-order kinetics plot with (left) and without (right) induction region and (b) second-order kinetics plot with and without induction region.

3.4. Ecotoxicity test

Assessing ecotoxicity by exposing brine shrimp to varying concentrations of AC and observing them after 24 hours is a method in ecotoxicology. Brine shrimps serve as suitable model organisms due to their sensitivity to environmental changes and toxins, as well as their ease of culture. The straightforward experimental procedures involve preparing solutions for different AC concentrations and monitoring brine shrimp mortality, providing a direct measure of toxicity. The method allows for the establishment of concentration-response relationships, facilitating the determination of lethal or effective concentrations. Table 2 summarizes the results for this test.

Based on the results in Table 2 and the LC_{50} bar chart in Fig. 6, the LC_{50} was calculated for AC with different weights. The estimated LC_{50} value of 33.11 from the ecotoxicity test indicates moderate toxicity of AC to brine shrimps, with 50% mortality within 24 hours at this concentration. Since the lethality test was conducted in about 10 mL of solution containing Artemia sp., the LC_{50} value can also be computed as 3311 mg/L. This finding is significant for assessing the ecological risk associated with AC use, particularly in aquatic environments, where it poses a substantial threat to aquatic life at or above this concentration. Evaluating this LC_{50} value against regulatory standards is imperative to ensure compliance with permissible toxicity levels for industrial applications. Further investigations involving diverse species and varying conditions are necessary to gain a comprehensive understanding of AC's environmental impact [20].

Table 2: Results of alive brine shrimp after 24 hours

Concentration of AC (mg)	Log concentration	No. of shrimps exposed	No. of fish died at 24 h	Percent kill [%]	Probit
20	1.301	20	8	40	4.75
30	1.477	20	9	45	4.87
50	1.689	20	12	60	5.25

The bar chart (Fig. 6) illustrates the percentage of brine shrimp mortality after exposure to different amounts of AC. Mortality increased with increasing AC dosage. At 20 mg AC, approximately 40% of the shrimp population died, while 30 mg AC resulted in about 45% mortality. The highest mortality rate, around 60%, was observed at 50 mg AC, indicating a dose-dependent toxic effect. In contrast, the negative control group, which received no AC, showed only about 20% natural mortality. These results demonstrate that higher concentrations of CFRP-derived AC are more toxic to *Artemia* sp., consistent with the calculated LC_{50} value.

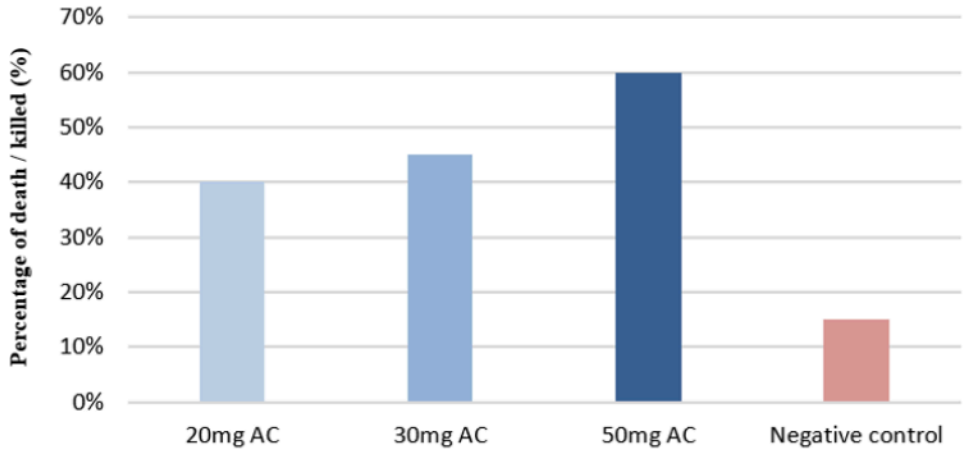

Fig. 6. Death percentage of brine shrimp after 24 hours exposed to AC.

Interestingly, the ecotoxicity assessment conducted using the *Artemia* sp. brine shrimp bioassay revealed a clear gap in the literature, no prior LC_{50} values have been reported for AC using this assay, including for those produced from CFRP waste. This gap appears to stem from the common assumption that AC is inherently safe due to its carbon-based composition, chemical stability, and general biodegradability. As a result, very few studies have investigated the lethal toxicity of AC toward aquatic organisms. However, despite its perceived safety, AC can still pose risks in aquatic environments. AC particles may interact physically with small organisms, alter water chemistry, interfere with respiration or feeding mechanisms, or adsorb essential nutrients, potentially leading to sub-lethal or lethal effects. Therefore, even though ecotoxicity testing of AC is limited in the literature, evaluating its impact on aquatic life remains important. In this study, we provide such data (as shown in Table 3) and include comparative information from related carbon-based materials, such as carbon nanotubes, that have been tested using the brine shrimp assay.

Table 3: Ecotoxicity (LC_{50}) comparisons for carbon-based Materials

Carbon materials	Test organism	Exposure time [h]	LC_{50} [mg/L]	Notes	Ref.
CFRP-derived AC (this study)	*Artemia* sp.	24	3311	First reported of AC LC_{50} via brine shrimp assay	-
Single-walled carbon nanotubes (SWCNTs)	*Artemia* sp.	24	509.25	Higher toxicity than AC in this study	[21]
Multi-walled carbon nanotubes (MWCNTs)	*Artemia* sp.	24	3750.51	Slightly lower toxicity than AC in this study	[21]

Table 3 presents the LC_{50} values of the CFRP-derived AC obtained in this study alongside reported LC_{50} values for related carbon-based materials tested using *Artemia* sp. The LC_{50} for the synthesized AC was determined to be 33.11 mg in 10 mL, corresponding to 3311 mg/L. This relatively high LC_{50} value indicates low acute toxicity, as a large amount of AC is required to induce 50% mortality in the brine shrimp population. For comparison, single-walled carbon nanotubes (SWCNTs) exhibit a lower LC_{50} (≈ 509 mg/L), reflecting greater toxicity toward *Artemia* sp. In contrast, multi-walled carbon nanotubes (MWCNTs) show a higher LC_{50} (≈ 3750 mg/L), indicating slightly lower toxicity than the AC tested in this work. These results demonstrate that the CFRP-derived AC falls within the lower-to-moderate toxicity range relative to other carbon-based nanomaterials evaluated using the same organism

4. CONCLUSION

AC was successfully synthesized from CFRP based on the presence of high oxygen-containing functional groups, such as (-OH and C–O), from FTIR analysis, a porous and irregular morphology with interconnected micropores and mesopores from SEM analysis, and a predominantly amorphous structure with minor graphitic domains from the XRD analysis. The Langmuir model provided the best fit (adjusted $R^2 = 0.88$) for the adsorption isotherm of the CFRP-derived AC, confirming monolayer adsorption capacity. The adsorption kinetics followed the pseudo-first-order model (adjusted $R^2 = 0.96$), suggesting that the adsorption rate is concentration-dependent. Ecotoxicity assessment using brine shrimp bioassays yielded an LC_{50} value of 33.11 mg (or 3311 mg/L), indicating moderate toxicity with 50% mortality within 24 hours. These results demonstrate that CFRP-derived AC possesses excellent adsorption capacity and acceptable ecological risk, making it a promising material for wastewater treatment and other industrial applications. This study also presents the first LC_{50} value for AC via the brine shrimp assay, addressing a key literature gap. Further research should assess regeneration, reusability, long-term stability in real wastewater, and production scalability for larger systems.

ACKNOWLEDGEMENT

As supervisor, Dr. Ricca Rahman Nasaruddin acknowledges Nik Misha Adrina Binti Nik Ahmad Shafrizal for her contributions to sample preparation, experimental work, data collection, analysis, and co-writing the draft of the article for her final-year project during her bachelor's degree. Dr. Ricca Rahman Nasaruddin also acknowledges Dr. Mariatul Fadzillah Mansor for her contribution in co-writing and reviewing the final revised

manuscript, and Dr. Nor Farah Huda Abd Halim for her contribution in supplying the CFRP wastes and providing insights for the CFRP properties and characterization.

REFERENCES

[1] Huda AHNF, Ascroft H, and Barnes S. (2016) Machinability Study of Ultrasonic Assisted Machining (UAM) of Carbon Fibre Reinforced Plastic (CFRP) with Multifaceted Tool. Procedia CIRP, 46:488-491.

[2] Butenegro JA, Bahrami M, Abenojar J, and Martínez MÁ. (2021) Recent Progress in Carbon Fiber Reinforced Polymers Recycling: A Review of Recycling Methods and Reuse of Carbon Fibers. Journal, 14(21): 10.3390/ma14216401

[3] Roberts T. (2006) The Carbon Fibre Industry: Global Strategic Market Evaluation 2006-2010. Watford, UK: Materials Technology Publications.

[4] Nahil MA and Williams PT. (2011) Recycling of carbon fibre reinforced polymeric waste for the production of activated carbon fibres. Journal of Analytical and Applied Pyrolysis, 91(1): 67-75.

[5] Vo Dong PA, Azzaro-Pantel C, and Cadene A-L. (2018) Economic and environmental assessment of recovery and disposal pathways for CFRP waste management. Resources, Conservation and Recycling, 133:63-75.

[6] Ullah S, Shah SSA, Altaf M, Hossain I, El Sayed ME, Kallel M, El-Bahy ZM, Rehman Au, Najam T, and Nazir MA. (2024) Activated carbon derived from biomass for wastewater treatment: Synthesis, application and future challenges. Journal of Analytical and Applied Pyrolysis, 179:106480.

[7] Patel A, Sharma D, Kharkar P, and Mehta D. (2019) Application of Activated Carbon in Wasterwater Treatment. International Journal of Engineering Applied Sciences and Technology, 3(12):63-66.

[8] Fathi FR, Amir D, Halim NFHA, and Nasaruddin RR. (2023) Investigating the Synthesis of Activated Carbon from Carbon Chips of Carbon Fibre Reinforced Polymer for the Removal of Methylene Blue. In: Maleque, M.A., Ahmad Azhar, A.Z., Sarifuddin, N., Syed Shaharuddin, S.I., Mohd Ali, A., Abdul Halim, N.F.H. (eds) Proceedings of the 5th International Conference on Advances in Manufacturing and Materials Engineering. Lecture Notes in Mechanical Engineering. Springer, Singapore.

[9] Eleryan A, Hassaan M, Nazir MA, Shah SSA, Ragab S, and El Nemr A. (2024) Isothermal and kinetic screening of methyl red and methyl orange dyes adsorption from water by Delonix regia biochar-sulfur oxide (DRB-SO). Scientific Reports, 14(1):13585.

[10] Amir D, Nasaruddin RR, Yousefi M, Mastuli MS, Sulaiman S, Alam MZ, and Engliman NS. (2024) Investigating the synthesis parameters of durian skin-based activated carbon and the effects of silver nanocatalysts on its recyclability in methylene blue removal. Discover Nano, 19(1):32.

[11] Enders AA, North NM, Fensore CM, Velez-Alvarez J, and Allen HC. (2021) Functional Group Identification for FTIR Spectra Using Image-Based Machine Learning Models. Analytical Chemistry, 93(28):9711-9718.

[12] Sutar RB, Kulkarni GK, Koli RR, Dhas SD, Velhal NB, Rajpure KY, Puri VR, and Yadav JB. (2025) Bio-derived graphitic carbon microspheres: A green approach for high-frequency microwave absorption. Diamond and Related Materials, 151:111836.

[13] He G, Ma X, Xu Z, Yan Z, Meng H, and Shen PK. (2011) Direct formation of nanostructured graphitic carbon from an acrylic ion-exchange resin at 600°C. Journal of Materials Research, 26(24):3083-3090.

[14] Sandeep A, T P, and Ravindra AV. (2024) Activated carbon derived from corncob via hydrothermal carbonization as a promising electrode for supercapacitors. Materials Research Bulletin, 179:112991.

[15] Ullah S, Rehman Au, Gurbanova L, Najam T, Al-Mohaimeed AM, Al-Onazi WA, Khan k, Shah SSA, and Nazir MA. Synthesis of MIL-88@activated carbon composite as an efficient adsorbent for the removal of Rhodamine B. International Journal of Environmental Analytical Chemistry:1-19.

[16] Sevim F, Laçin Ö, Demir F, and Erkiliç ÖF. (2025) Adsorption Capacity, Isotherm, Kinetics, and Thermodynamics Examinations on the Removal of a Textile Azo Dye by Local Natural Adsorbent. Global Challenges, 9(5):2500024.

[17] Gupta SA, Vishesh Y, Sarvshrestha N, Bhardwaj AS, Kumar PA, Topare NS, Raut-Jadhav S, Bokil SA, and Khan A. (2022) Adsorption isotherm studies of Methylene blue using activated carbon of waste fruit peel as an adsorbent. Materials Today: Proceedings, 57:1500-1508.

[18] Hoc Thang N, Sy Khang D, Duy Hai T, Thi Nga D, and Dinh Tuan P. (2021) Methylene blue adsorption mechanism of activated carbon synthesised from cashew nut shells. RSC Advances, 11(43):26563-26570.

[19] Eregowda T, *Anaerobic Treatment and Resource Recovery from Methanol Rich Waste Gases and Wastewaters*. 1st ed. 2019, CRC Press: CRC Press.

[20] Nunes BS, Carvalho FD, Guilhermino LM, and Van Stappen G. (2006) Use of the genus Artemia in ecotoxicity testing. Environmental Pollution, 144(2):453-462.

[21] Mohamadhossein F, Sadeghi MS, Emtyazjoo M, and Seyedi J. (2023) Comparative toxicity of single-wall and multi-wall carbon nanotubes to brine shrimp Artemia salina Research in marine Sciences, 7(2):17-30.